

DESIGN AND EVALUATION OF AN IDEALIZED POROUS MEDIUM FOR CALIBRATION OF PERMEABILITY MEASURING DEVICES

Andrew P. Vechart¹, Reza Masoodi and Krishna M. Pillai*

Laboratory for Flow and Transport Studies in Porous Media, Department of Mechanical Engineering, University of Wisconsin-Milwaukee, EMS, 3200 N. Cramer St., Milwaukee, WI 53211, USA
<http://www4.uwm.edu/porous/>

Currently pursuing M.Sc. in Computation for Design and Optimization Program at M.I.T.

*Author to whom correspondence should be addressed

E-mail: krishna@uwm.edu

Received 5 December 2009; accepted 17 December 2009

ABSTRACT

Calibration of permeability measuring devices or experimental setups remains an important concern of the flow modeling community of LCM processes (the set of technologies, including RTM and VARTM, that are used for manufacturing polymer composites) since the fidelity of any mold-filling simulation depends on the accuracy of fiber-mat permeability measured through experiments. The design and evaluation of a new cost-effective and accessible calibration-tool for use in both 1-D and radial flow set-ups used in the permeability evaluation experiments is presented here. The tool, comprising of a lattice-like structure patterned out of a repeating unit-cell and based on the design proposed by Morren *et al.* [9], represents an idealized porous medium of known permeability that can be used for such calibrations. Stereolithography technique was used to manufacture the tool out of a plastic to fine tolerances. Computational fluid dynamics (CFD) simulations were then performed in the unit cell to evaluate the principle permeabilities of the idealized porous medium. Thereafter, the proposed calibration tool was used in our experimental apparatus to evaluate the accuracy of our permeability measurements. The tool was used for the estimation of accuracy of *four* different methods: the transient and steady-state tests for the 1-D flow device, and the transient and steady-state tests for the radial flow device. Results show close agreement between the permeabilities estimated through experiments and the permeabilities estimated from the CFD simulation. The study thus establishes the usefulness of the idealized porous medium for calibrating permeability measuring devices.

Keywords: calibration, permeability, permeability measurement, mold-filling, LCM, RTM, VARTM, 1-D flow, radial flow, Darcy's law.

1. INTRODUCTION

The research presented here pertains to the calibration and validation of one-dimensional and radial flow experimental apparatus used to evaluate the permeability of fibermats used in the making of fiber-reinforced composites. Fibers made from glass or carbon are often used as reinforcements in composites. Such composite materials are popular as engineering materials particularly due to their high strength-to-weight ratio.

There are several ways to manufacture such composites. One broad class of such methods is known as the liquid composite molding (LCM) processes, which include resin transfer molding (RTM), vacuum-assisted resin transfer molding (VARTM), Seeman composite resin infusion molding process

(SCRIMP), and others. These processes saturate the reinforcement by either injecting matrix material into the reinforcement at the inlet of the mold, or by drawing matrix material into the reinforcement by pulling a vacuum at the outlet of the mold, or by a combination of both. Simulations are used in the mold design phase to determine positions of gates, vents, inlets, and outlets and such parameters as the injection temperature of the resin. Validity of these simulations depends highly on the accuracy of reinforcement permeability, which can vary along different flow directions in a given anisotropic material [1, 2]. It is often difficult to estimate the permeability of a reinforcement via computational fluid dynamics methods; hence, permeability values for a porous material are often determined experimentally.

In the research presented here, two different experimental methods for determining permeability of porous media are considered, the one-dimensional flow method and the radial flow method. (Details of these methods are presented in the Theory section.) While these methods are theoretically well established, the experiments are subject to several sources of variability. Hoes *et al.* [3] lists some of these sources, including “deformation of the material during sample preparation (shearing)”, “random experimental errors”, “existence of micro-flow within yarns”, “material heterogeneity due to manufacturing”, and “uncontrolled nesting of layers during stacking and compression of the multi-layered samples”. Such variations can result in large unpredictability in experimental results, thereby possibly invalidating the aforementioned LCM flow-modeling simulations based on the permeability values obtained through these experiments.

Not only is there uncertainty of results from these experiments due to the variability mentioned previously, but the suitability of the experimental set-up itself can be questioned as well. Currently, there is no universally accepted method to calibrate or validate one-dimensional or radial flow experimental set-ups used to determine permeability of porous media. While experimenters in different labs may make careful efforts to ensure the performance of their equipment, currently the only way to compare the accuracy of different set-ups is to run experiments on the same porous medium and compare the results. However, these results are subject to the variability already discussed, and they may provide confusing conclusions.

There have been efforts to find an acceptable standard reference material for equipment calibration. Parnas *et al.* in [4] analyzed a 3-D woven fabric using both one-dimensional and radial flow tests for suitability as a reference material. Even though the measurements were done with high precision, the repeatability of estimated permeabilities was around 15%. While the material was received with accurate tow-level geometrical features, experiments were still subject to variability from edge effects induced by preparatory cutting of the material [4]. Another

effort to provide a reference point for the evaluation of fiber-mat permeability was put forth by the National Institute of Standards and Technology (NIST) as described in [5]. In well-defined, controlled experiments, the permeabilities of several types of glass fabrics were evaluated and made available in a database format. Despite the standardization of experiments and reference materials, permeabilities listed in the database had large uncertainties, in some cases reaching $\pm 50\%$ [5].

Lundstrom *et al.* in [6] presented a remarkable 1-D flow based experimental method to evaluate the full in-plane permeability tensor of an anisotropic fiber mat in a single constant-injection-pressure experiment. The mold for these experiments consisted of four cavities, three for three different orientations of the material and one for a bank of capillary tubes serving as a reference material. Repeated permeability measurements using this method had a standard deviation of 10%; however, these experiments were still subject to many of the sources of variability mentioned previously.

Roy *et al.* [7] proposed a method to calibrate 1-D flow experimental set-ups using a reference medium composed of an aluminum plate with a series of small, aligned holes with tightly controlled radial dimensions. The theoretical and numerical permeabilities of the medium were ascertained using the Hagen-Poiseuille flow equation and Fluent[®], respectively. For the set-up considered, it was shown that the experimentally measured permeability values agreed with the exact (numerical and theoretical) values at low flow rates. The rigid nature of the reference medium led to deviations from the exact value at higher injection-rates due to mold deflection; however, such deviations in setup accuracy with flow rate was not experienced by the normal glass-fabrics since expansion in the mold thickness was compensated by expansion in the pre-compressed glass-fiber mats [7]. Later, Hua *et al.* [8] developed an affordable reference material consisting of concentric, annular slits for radial-flow setup. A similar increase in inaccuracy with increasing flow rate was observed for this reference material as well due to an increase in mold deflections at higher flow rates.

Morren *et. al.* [9] developed and tested an idealized porous-medium manufactured through stereo-lithography as a rigid reference-material for their radial-flow based permeability measuring device. The lattice-like material was created by repeating a unit-cell structure such that the unit-cell dimensions were much smaller than the medium dimensions. Since the flow of resin-like test fluid through the medium correspond to the inertia-less low Reynolds number flow regime, the exact permeability of the reference medium was estimated by evaluating the permeability of the unit cell through CFD. Details of the unit cell used for creating the reference material are shown in Figs. 1 and 2a [9, 10].

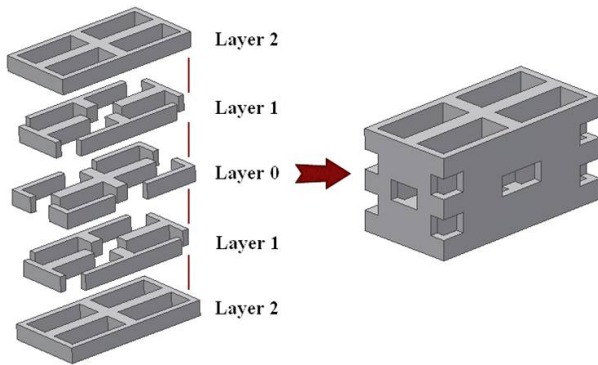
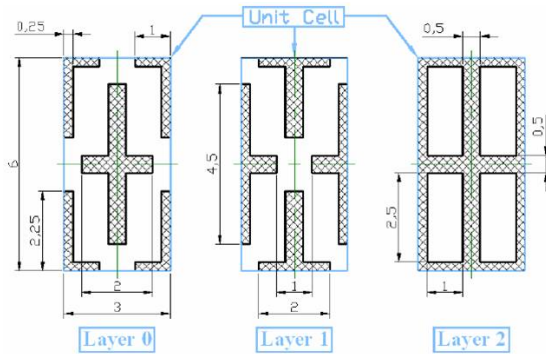
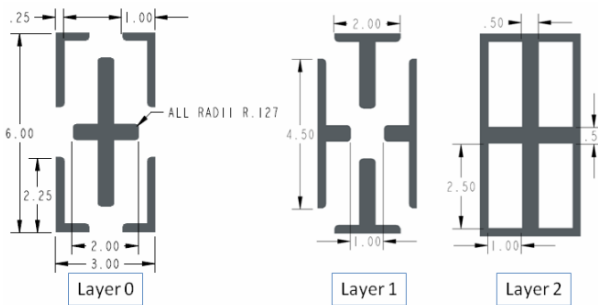


Fig. 1: Detailed view of the original layered unit-cell structure developed by Morren *et al.* [9] for their idealized reference (porous) medium.



a) The original structure developed by Morren *et al.* [9].



b) The modified structure used in the present study.

Fig. 2: Dimensions (in mm) of the unit-cell structures employed for creating idealized reference (porous) media.

In this paper, we adopt the unit-cell design of Morren *et. al.* [9] to create a reference (idealized) porous medium for calibrating *both* 1-D flow and radial flow based permeability measurement devices. Presented here is a validation of the previous work followed by a description of the adaptation of this reference medium for both the 1-D and radial flow set-ups used in our lab. For the first time, such a medium is being used to estimate the accuracy of *four* different but well-known methods of permeability estimation, leading to a more in-depth analysis of its effectiveness and potential as a future standard for calibration of permeability measuring devices.

2. MATHEMATICAL THEORY

2.1 Darcy's Law

Because it is practically impossible to recreate the structure of the fiber reinforcements used in LCM process for point-wise flow modeling through CFD (and computationally expensive to create a mesh fine enough to capture the true flow-characteristics in a porous medium consisting of thousands of pores), LCM mold-filling simulation software calculate volume-averaged flow characteristics through such porous media using Darcy's Law [Eq (1)] as

$$q = -\frac{\mathbf{K}}{\mu} \cdot \nabla P \quad (1)$$

where

$$\mathbf{K} = \begin{bmatrix} K_{xx} & K_{xy} \\ K_{yx} & K_{yy} \end{bmatrix} \quad (2)$$

Here the vector q represents the in-plane Darcy velocity, the symbol ∇P represents the pressure gradient, and μ represents the dynamic viscosity of the resin or test liquid. The tensor \mathbf{K} represents the permeability of an anisotropic porous medium. (Since structure of the reference medium unit-cell is different along its two principal directions, the idealized porous medium created by the reference medium is anisotropic.) \mathbf{K} shown above is in general two-dimensional tensor form; however, it is a symmetric second-order tensor and can be written with its off-diagonal components equal to zero when expressed in its principal coordinate system.

Note that the use of Darcy's Law is valid only for

low pore-based Reynolds numbers (i.e. $Re < 1$) corresponding to inertia-less creeping flows. Such a pore-based Reynolds number is defined as

$$Re = \frac{\rho q d}{\mu} \quad (3)$$

where ρ represents the liquid density, d is the characteristic width of the porous-medium flow-channels that can be estimated as the square root of the porous-medium permeability (i.e., $d \approx \sqrt{K}$).

2.2 1-D Flow

The one-dimensional (1-D) flow experiment allows for estimation of the permeability of a material along the particular direction of the material aligned with the direction of flow (see Fig. 3). A rectangular closed mold contains one or more layers of the reinforcement material of interest. A test fluid of known viscosity is then injected into the mold at either constant (known) pressure or at a constant (known) flow rate. If injected at constant pressure, the flow rate through the material is measured. If injected at a constant flow rate, the pressure drop across the material is measured.

Typical experiments to measure in-plane fiber-mat permeability

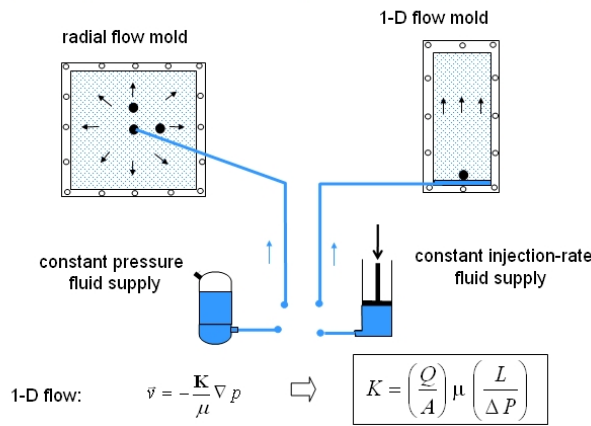


Fig. 3: A schematic depicting the general set-up for the radial and one-dimensional permeability evaluation experiments.

For a *steady-state* estimation of permeability, the one-dimensional form of Darcy's Law is used as

$$\frac{Q}{A} = \frac{K_{ss}}{\mu} \frac{P_{inlet} - P_{outlet}}{L} \quad (4)$$

where Q represents the flow rate through the reference medium, A is the frontal cross-sectional area of the reference medium, P is the pressure, L is the

length of the material, and μ is the dynamic viscosity of the fluid. The variable K_{ss} is the steady-state permeability of the material along the flow direction.

An estimation of permeability under transient mold-filling conditions can be performed as well; such a permeability is referred to as the *transient* permeability. Because both the flow-front position and inlet pressure have a linear relationship with time in a constant flow-rate experiment, the following relationship (assuming the outlet pressure to be atmospheric) holds.

$$K_{tr} = \frac{V_{front}^2 \cdot \mu \cdot \varepsilon \cdot t}{P_{inlet}(t)} \quad (5)$$

Here V_{front} is the velocity of liquid flow-front traveling in a 1-D flow mold, t is the time since the liquid began penetrating the medium, and P_{inlet} is the pressure at the inlet side of the medium as a function of time. Note that the unsaturated flow effects, which typically appear near the flow-front in fibrous reinforcements during the transient mold-fillings due to the surface tension effect or dual-scale effect, are absent in our reference medium due to its relatively larger pores (Figs. 1, 2 and 5).

2.3 Radial Flow

The radial flow experiment (shown in Fig. 3) allows for estimation of both the principle permeability values and their orientations. A test fluid at a constant flow-rate is injected into the center of a square preform composed of the fiber mats tacked on top of each other. For an isotropic material, the flow-front is circular, while for an anisotropic material, the flow-front is elliptical during the transient mold-filling process. In terms of the principle permeabilities, a *transient* permeability can be estimated [11,12,13] through the equations

$$K_{eff} = \frac{\mu Q}{2\pi h P_{inlet}} \left[\ln \left(\frac{r_{l,front}}{r_0} \right) + \ln f \right] \quad (6)$$

where

$$f = \frac{1 + \sqrt{1 + \frac{r_0^2}{r_{l,front}^2} \left(\frac{1}{\alpha} - 1 \right)}}{\frac{\sqrt{\alpha + 1}}{\sqrt{\alpha}}} \quad (7)$$

$$\alpha = \left(\frac{r_{2,front}}{r_{1,front}} \right)^2 = \frac{K_2}{K_1} \quad (8)$$

In these equations, h is the thickness of the preform in the mold, $r_{1,front}$ is the radius of the elliptical flow-front along the major axis, $r_{2,front}$ is the radius of the elliptical flow-front along the minor axis, r_0 is the inlet radius, K_1 is the first principle permeability, and K_2 is the second principle permeability [11,12,13].

In the transient radial-flow experiment, α can be determined from the shape of the elliptical flow-front. The slope of the plot of inlet pressure versus the quantity in brackets in Eq (6) can then be substituted into Eq (6) to calculate the effective permeability. The principle permeabilities [11,12,13] can then be found as

$$K_{eff} = \sqrt{K_1 K_2} \quad (9)$$

$$K_1 = \frac{K_{eff}}{\sqrt{\alpha}} \quad (10)$$

$$K_2 = K_{eff} \sqrt{\alpha} \quad (11)$$

Note once again that the unsaturated flow effects, which typically appear near the flow-front in fibrous reinforcements during the transient mold-fillings due to the surface tension effect or dual-scale effect, are absent in our reference medium due to its relatively larger pores.

In addition to the method described above, the permeability characteristics of a reinforcement can be estimated through a *steady-state* radial-flow analysis as proposed by Han et al. [14]. Followings are the suggested relations to estimate the permeability from the pressure and flow-rate measurements under steady-state conditions [14].

$$\ln \left[\sqrt{\left(\frac{x_1}{r_0} \cdot \frac{I}{\sqrt{1-\alpha}} \right)^2 - I} + \frac{x_1}{r_0} \frac{I}{\sqrt{1-\alpha}} \right] - \ln \left[\frac{1+\sqrt{\alpha}}{\sqrt{1-\alpha}} \right] - \frac{2\pi h(P_0 - P_1)}{Q\mu} K_{eff} = 0 \quad (12)$$

$$\ln \left[\sqrt{\left(\frac{y_2}{r_0} \cdot \frac{\sqrt{\alpha}}{\sqrt{1-\alpha}} \right)^2 + I} + \frac{y_2}{r_0} \frac{\sqrt{\alpha}}{\sqrt{1-\alpha}} \right] - \ln \left[\frac{1+\sqrt{\alpha}}{\sqrt{1-\alpha}} \right] - \frac{2\pi h(P_0 - P_2)}{Q\mu} K_{eff} = 0 \quad (13)$$

These equations assume there is a pressure transducer at the center of the preform (P_0), a pressure transducer on the global x-axis (P_1), and a pressure transducer on the global y-axis (P_2) (see Fig. 4). In these equations, r_0 is the radius of the inlet, x_1 is the x-coordinate of the first pressure transducer, y_2 is the y-coordinate of the second pressure transducer, h is the thickness of the preform, and Q is the constant volumetric flow-rate of the test fluid. Using the pressure and flow rate data collected during steady-state operation of the radial flow experiment, Eqs (12) and (13) can be solved simultaneously for α and K_{eff} , which are defined according to Eqs (8) and (9). These values can then be substitute into Eqs (10) and (11) to find the principle permeability values [14].

3. DESIGN AND MANUFACTURING OF RIGID CALIBRATION TOOL

3.1 Validation of the Previous Design Through Fluent® Simulations

The values for the principle permeabilities of the unit-cell structure adopted for the present work are listed by Morren et al. [9]. To validate these values, the unit-cell structure shown in Figs. 1 and 2a was modeled in Gambit® and, subsequently, a flow analysis was performed in Fluent® along both the principle directions. For a prescribed pressure dif-

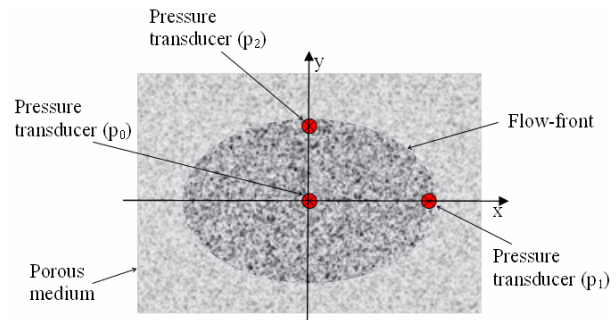


Fig. 4: A schematic showing the moving flow-front and location of transducers for the radial-flow experiment.

ference across the unit cell, the volumetric flow-rate was evaluated. Then, Eq (4) was used to estimate the permeability along the flow direction. Sensitivity studies were also performed to validate the method of extending the permeability of a single unit-cell to that of a bulk material composed of several unit-cells. Similarly, a sensitivity study was performed to analyze the effect of the side walls of the one-dimensional experimental apparatus on the flow through the reference material; it was observed that such wall effects are minimal.

In Table 1, the cited principle permeability values for the unit cell are listed along with values obtained through the CFD simulations. As can be seen from the table, results for K_1 from simulation closely match that listed in the literature [9]. The observed small discrepancy is expected. The results for K_2 show a higher percentage discrepancy. However, in terms of absolute differences, the discrepancy in K_2 is on the same order of magnitude as in K_1 . These discrepancies can perhaps be attributed to the use of different CFD software used by Morren et al. and us for the unit-cell flow simulation.

Table 1: Comparison of the cited permeability values of a unit cell from reference [9] and the Fluent® simulation results for the original unit-cell.

	units	Cited	Simulation	Difference
K_1	10^{-9} m^2	4.8	4.6	4.2%
K_2	10^{-9} m^2	1.4	1.9	35.7%

3.2 Designing a Calibration Tool for 1-D Flow Experiments

The one-dimensional flow experiment requires a rectangular reference-medium of the same width and thickness as the mold cavity. The mold cavity used for these experiments has a width of 177.80 mm (7.00 in) and thickness of 9.53 mm (0.375 in). Therefore, the designed medium was quite simply a rectangular array of unit cells all in the same orientation. To facilitate evaluation of permeability along both directions, the material was composed of an almost square matrix of 29 unit cells by 59 unit cells. This left the material slightly smaller than the mold cavity width. This gap was to be filled with a gasket as described in section 4.1. Similarly, the thickness of the material was less than the thickness

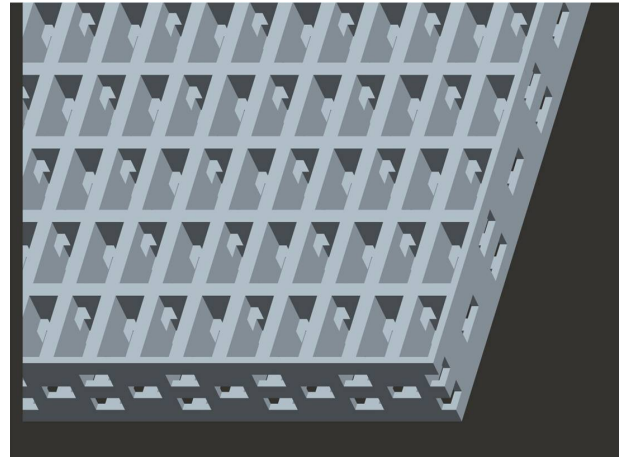


Fig. 5: Magnified details near the corner of the unit-cell based calibration tool.

of the mold cavity. Again, this gap was occupied by gaskets as described in section 4.1. Fig. 5 shows a 3D rendering of several unit-cells combined to form the tool.

3.3 Designing a Calibration Tool for Radial Flow Experiments

To reduce cost and manufacturing time, it was desired to adapt the reference part used in the one-dimensional experiment for use in the radial-flow experiment as well. The radial-flow experiment requires a circular preform. A circular adapter was created with a rectangular hole for the one-dimensional experiment part. The adapter was created with complete unit cells to preserve the strength of the structure. Therefore, the edges of the circular adapter were stepped instead of smooth. However, deviations from a smooth circular outer circumference were small and were not expected to have a large effect on the permeability measurement results. A 3-D rendering of the adapter can be seen in Fig. 6.

3.4 Manufacturing of the Designed Calibration Tools

Rapid prototyping techniques are invaluable engineering tools allowing for quick and, in general, inexpensive manufacturing of parts both for design analysis and for operational use. Often these processes are capable of producing features that require high precision. Stereolithography is an additive rapid-prototyping process whereby a UV laser passes over a bed of photopolymer resin, solidifying

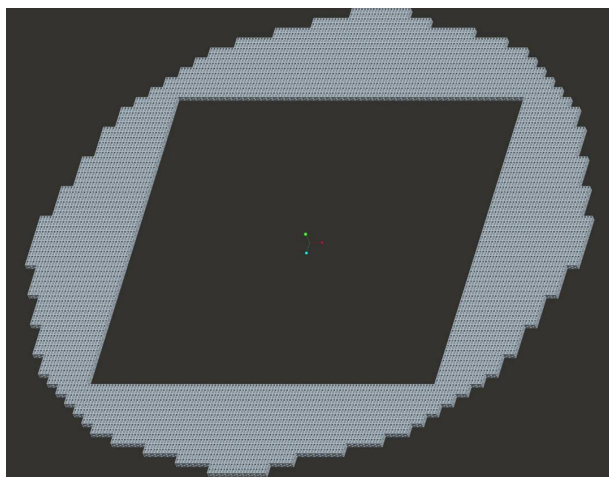


Fig. 6: Circular adapter used during the radial-flow tests.

the full part layer-by-layer until the part is complete [10]. The additive nature of this process allows for creation of complex internal geometries that cannot be made through subtractive processes such as machining.

The reference medium tested in this research was manufactured on a commercial Viper Pro[©] stereolithography machine. This process used a 1000 mW laser of beam diameter 0.005 in (0.127 mm) [15]. Note that some alterations were made to the original unit-cell design (Fig. 1 and 2a) proposed by Morren et al. [9]. The external corners were rounded (Fig. 2b) to account for the finite diameter of laser beam used during the stereolithography process. The material used was Accura 60 plastic, having a listed hardness of Shore D 86 [15]. The company that manufactured the part was able to do so in less than a week at a total cost of approximately \$400, making this tool very accessible and relatively cost-effective.

4. EXPERIMENTAL PROCEDURE

4.1 One-Dimensional Flow Experiment

The main test-bed for the one-dimensional flow experiments was a rectangular aluminum block machined out to accommodate rectangular test-preforms. For these experiments, layers of gaskets were laid in the mold followed by the rectangular portion of the calibration tool. As mentioned in section 3.2, the tool was thinner than the mold-cavity thickness. To fit the tool in the mold cavity, two Buna-N rubber gaskets (having durometer A60) were used. Be-



a) 1-D flow set-up

b)



c) Radial flow set-up

d)

Fig.7: 1-D and Radial flow set-ups with installed pressure-transducers

cause flow-front visualization is necessary for transient permeability estimations, the gasket between the tool and the top sealing-plate in both experimental set-ups was a transparent silicone-rubber gasket (having durometer 40A). During experiments, it was verified that the hardness of this gasketing combination was appropriate to adequately seal the tool in the closed molds. Additionally, thin strips of the Buna-N gasket material were used to fill in the side-wall gaps for the one-dimensional experiments. A 2.54 cm thick Lexan plate then sealed the preform within the aluminum mold. Finally, a thick aluminum frame was placed over the Lexan plate, and the frame was bolted to the mold. Additional supports and large C-clamps were put in place to prevent mold deflection during filling. Fig. 7a shows the base, Lexan plate, and frame assembled.

Motor oil (SAE 10W-40) was injected into one side of the mold through a reinforced hydraulic hose, minimizing the pressure-relief effects due to hose expansion. Viscosity of the oil was assessed with a Brookfield[®] Viscometer. At the opposite end of the mold was a drain open to atmospheric pressure. Oil injection was achieved via a gear pump driven by a stepper motor in a closed-loop feedback control

scheme with a flow meter as the input.

Pressure data from the experiment was collected via a transducer inserted into the Lexan plate on the inlet side of the preform (see Fig. 7a). This data was gathered by a LabView® data acquisition software via a 16-channel data logger (National Instruments TBX-68) [16]. Also, the flow front progression was video recorded for the transient flow-analysis.

4.2 Radial Flow Experiment

The radial-flow experimental platform consisted of a square Lexan plate base. Gaskets were laid on top of this base to the appropriate thickness. Next, the calibration tool (consisting of the rectangular part laid within the circular adapter) was laid on top of these gaskets. Finally, a clear gasket was placed over the calibration tool. A metal spacer of appropriate thickness was inserted on the perimeter of the based, and another square Lexan plate sealed the preform in the mold. The mold was bolted together around the perimeter along with angle-aluminum braces to increase mold stiffness. Additionally, large C-clamps were put in place to further minimize mold deflection. Fig. 7b shows the mold for radial-flow experiments.

Motor oil (SAE 10W-40) was injected into the center of the base Lexan plate through a hydraulic hose, minimizing the pressure-relief effects due to hose expansion. Viscosity of the oil was assessed with a Brookfield® Viscometer. There was a drain near the outer edge of the mold open to atmospheric pressure. Oil injection was achieved via a gear pump driven by a stepper motor in a closed-loop feedback control scheme with a flow meter as the input.

Pressure data from the experiment was collected via three pressure transducers inserted into the top Lexan plate (Fig. 7b). Holes were cut in necessary places in the gaskets to allow fluid to pass into the mold and to allow fluid to reach the pressure transducers. This data was gathered by a LabView® data acquisition software via a 16-channel data logger (National Instruments TBX-68) [16]. Also, the flow front progression was video recorded for the transient flow-analysis.

5. CALIBRATION TOOL EVALUATION

5.1 Modification in the Idealized Unit-Cell Geometry

The prescribed unit-cell geometry for the calibration tool consists entirely of sharp edges (Figs. 1 and 2a). However, as described before, the stereolithography process involves a laser of finite beam-diameter solidifying the polymer resin. Therefore, it is physically impossible to create perfectly-square external corners. Since permeability is a function of geometry, appropriate modifications to the fluid model considering laser-beam diameter (0.127 mm) [15] and model build-direction were made (Fig. 2b). The simulation was redone as described in section 5.3. with the modified geometry, and the results are shown in Table 2. The effect of this simple geometrical consideration is apparently significant. A comparison of the CFD simulation results for the original and modified media in Table 2 indicates that the inclusion of round edges changed both the principal permeabilities, K_1 and K_2 , by 87% and 157%, respectively.

Table 2: Comparison of the cited permeability values of a unit cell from reference [9] and the Fluent® simulation results for the modified unit-cell.

	units	Cited	Simulation	Difference
K_1	10^{-9} m^2	4.8	9.0	87.50%
K_2	10^{-9} m^2	1.4	3.6	157.14%

5.2 Porosity of the Designed Calibration Tool

An informative quantity characterizing a porous media is known as its porosity, which is the ratio of volume of empty space within the material to the total volume of the material. This is particularly useful for validation of the calculated flow-front velocity in the one-dimensional transient flow experiment. Knowing the porosity of the material, geometry of the preform, and volumetric flow rate, the theoretical flow front velocity can be ascertained with

$$V_{front} = \frac{Q}{\varepsilon A} \quad (14)$$

Here, V_{front} is the flow-front velocity, ε is the porosity of the material, and A is the flow-front cross-sectional area. Based on a volume analysis of a 3-D model of the reference medium (modified appropriately as discussed in section 5.1), the porosity of the

material was found to be 0.633.

5.3 CFD Evaluation Of The Calibration Tool

As previously indicated, an important feature of this proposed calibration tool or reference medium is the basic structure of its unit cell. Numerical evaluation of the permeability of the overall tool requires only the numerical evaluation of a single unit-cell. In the simulations for this work, the fluid domain within and around the unit-cell was modeled and meshed in the preprocessor Gambit[®]. No-slip boundary conditions were prescribed on all walls of the unit cell and at the surfaces that would be contacting the gaskets on top and bottom of the mold. Symmetry boundary conditions were imposed on the fluid surfaces having normal directions perpendicular to the direction of flow. The “inlet” and “outlet” fluid faces were open to larger “inlet” and “outlet” fluid volumes of prescribed pressure. By prescribing this pressure difference across the unit cell, the total flow-rate through the inlet or outlet faces could be numerically estimated and entered into Darcy’s Law, Eq (4), to obtain the estimated permeability value for the direction of flow considered. This analysis was performed along both principle directions of the unit cell.

Fig. 8 shows a velocity magnitude plot for a typical numerical simulation. The mesh was made fine

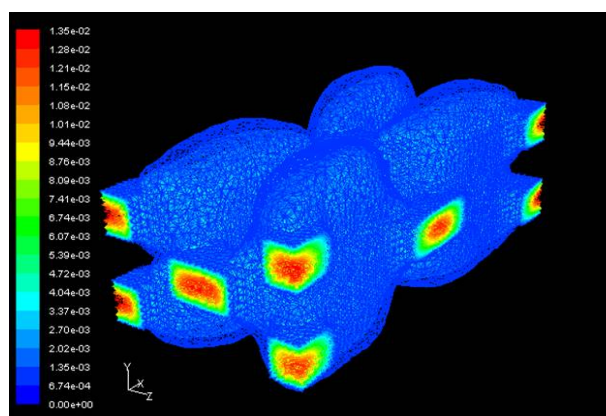


Fig. 8: Velocity plot from a typical CFD simulation generated by Fluent[®]

enough to capture the effect of the rounded edges resulting from the finite beam diameter of the laser as well as the no-slip boundary effects, typically having about 200,000 elements. The standard pressure differential used for the analysis was 10,000 Pa, yielding Reynolds numbers for the analysis to be around 0.2. Since this pore-based Reynolds number is less than unity, the presented CFD analysis is suitable for the Darcy’s law based inertia-less flow-regime seen in LCM processes.

6. EVALUATION OF REFERENCE-MEDIUM PERMEABILITY: RESULTS AND DISCUSSION

Tables 3 and 4 summarize the permeability evaluation results based on the four experimental proce-

Table 3: Experimentally determined permeability values for K_1

	No. of Trials	Average $K_1 [10^{-9} \text{ m}^2]$	Standard Deviation $[10^{-9} \text{ m}^2]$	Difference from CFD simulation
CFD Simulation		9.0		
1-D Transient	4	8.6±3.7	2.3	-4.8%
1-D Steady-State	21	9.5±0.8	1.7	5.6%
Radial Transient	2	8.8±7.4	0.8	-2.2%
Radial Steady-State	2	20.0±38.6	4.3	122.2%

Table 4: Experimentally determined permeability values for K_2

	No. of Trials	Average $K_2 [10^{-9} \text{ m}^2]$	Standard Deviation $[10^{-9} \text{ m}^2]$	Difference from CFD simulation
CFD Simulation		3.6		
1-D Transient	4	4.0±1.1	0.7	11.1%
1-D Steady-State	18	3.6±0.2	0.3	0%
Radial Transient	2	4.1±4.1	0.4	13.9%
Radial Steady-State	2	4.1±4.1	0.5	13.9%

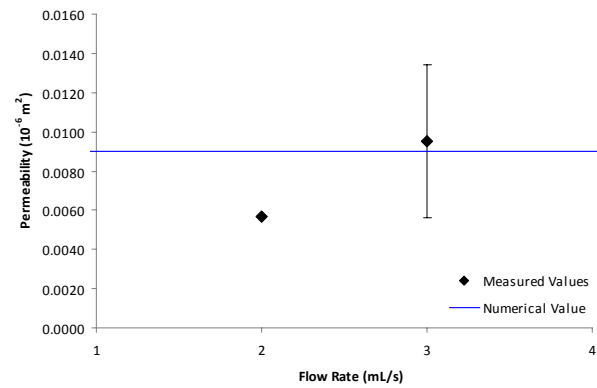
dures defined previously. The average values provided are listed with limits calculated based on a Student's t-test with a 95% confidence interval [17]. The sample standard-deviations used in calculation of the error limits are also listed.

Note in Tables 3 and 4 the number of trials in general led to the very conservative limits from the Student's t-test error estimations. For each transient one-dimensional permeability evaluation test, multiple steady-state tests could be conducted. Time constraints prevented additional radial evaluation tests, though results obtained are included here as initial indications of the outcomes of further tests.

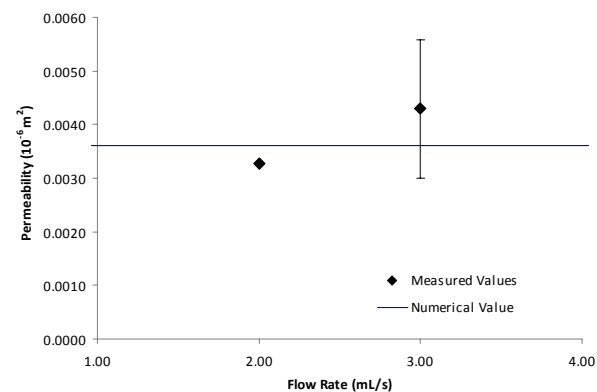
6.1 One-Dimensional Permeability Evaluations

1-D flow tests for permeability evaluation were performed on both principle directions of the test material. Results from the individual transient-flow experiments are shown in Figs. 9a and 9b. Error bars for each data point are provided based on 95% confidence interval. From these charts and the information in Tables 3 and 4, it can be seen that calculated permeabilities based on the one-dimensional transient experiments were consistent with those values estimated through CFD simulations. More data points are necessary to make this conclusion statistically significant, though relative consistency through these results supports the observation given here.

Furthermore, for the one-dimensional transient-flow evaluations, one can compare the results of the flow-front velocity used in calculations with the



a) Measured K_1 values versus flow-rate



b) Measured K_2 values versus flow-rate

Fig. 9: Measured principal-permeability values from the transient 1-D flow tests

theoretical flow-front velocity given by Eq 14. This comparison is given in Tables 5 and 6; these tables also provide the permeability values calculated for each trial. A general agreement can be seen between the measured and theoretical flow-front velocities. These results validate the flow-front velocities used in the 1-D transient-flow permeability evaluations. It can be seen that the calculated permeabilities fluctuate around the Table 2 values estimated from sim-

Table 5: Comparison of the measured and theoretical flow-front velocities for K_1 evaluation using the transient 1-D flow method

	units	Trial 1	Trial 2	Trial 3	Trial 4
Measured Front Velocity	mm/s	8.8	11.1	10.1	5.9
Theoretical Front Velocity	mm/s	8.9	8.9	8.9	6.0
K_1	10^{-9} m^2	7.8	10.1	10.8	5.7

Table 6: Comparison of the measured and theoretical flow-front velocities for K_2 evaluation using the transient 1-D flow method.

	units	Trial 1	Trial 2	Trial 3	Trial 4
Measured Front Velocity	mm/s	9.3	9.8	9.7	6.6
Theoretical Front Velocity	mm/s	9.1	9.1	9.1	6.1
K_2	10^{-9} m^2	3.8	4.2	4.9	3.3

ulations. This reaffirms our conclusion made earlier that the unsaturated-flow effects near flow-fronts can be neglected in the reference medium.

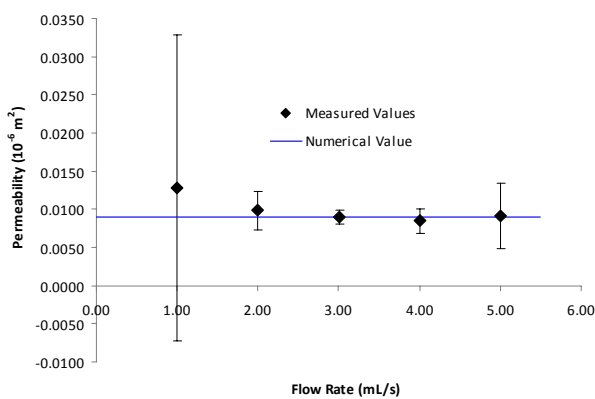
Results from individual steady-state one-dimensional experiments are shown in Figs. 10a and 10b. From these charts and the information in Tables 3 and 4, it can be seen that calculated permeabilities based on these experiments show good agreement with permeability values obtained from CFD simulations. The simulation values lie within the 95% confidence interval calculated for both the principle permeability values. From Figs. 10a and 10b, a consistent clustering of the experimental permeability values around the simulation values can be noticed.

Fig. 10a shows a larger scatter in the calculated K_1 values for lower flow rates, though this same characteristic is not seen in Fig. 10b for calculated K_2 values. According to the Darcy's Law, lower flow-rates mean lower pressures on the measurement side of the reference medium. The pressure transducers

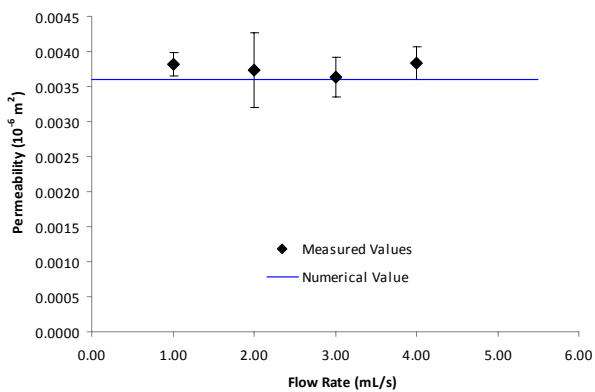
used for these experiments lose sensitivity at very low pressures, possibly leading to this discrepancy. This phenomenon is not seen for the same flow rates for the K_2 values because for the same flow rate, a lower permeability ($K_2 < K_1$) leads to a higher pressure. This also provides a possible explanation for the discrepancy in results between simulation and experiment for the 1-D transient permeability evaluations.

6.2 Radial Permeability Evaluations

Radial permeability evaluation tests were performed on the reference medium, allowing simultaneous calculation of both the principle permeability values. Results from the individual transient experiments are shown in Figs. 11a and 11b. Though limited trials were performed, the results of these experiments show positive agreement with the values obtained in simulations and are worth noting here. The error estimates in Tables 3 and 4 are very large based on the 95% confidence interval Student's t-test, due chiefly to the small number of trials. However, the

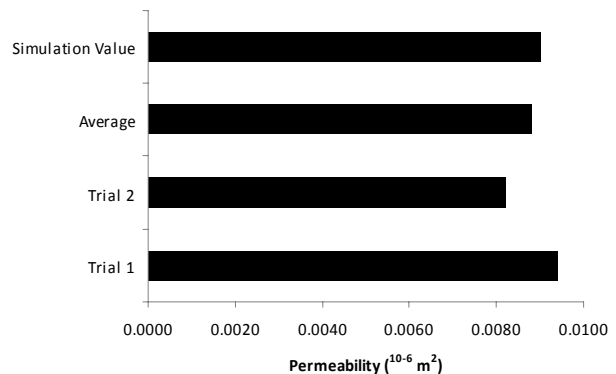


a) Measured K_1 values versus flow rate

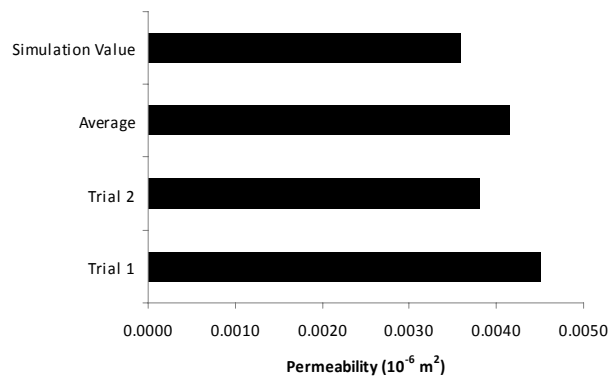


b) Measured K_2 values versus flow rate

Fig. 10: Measured principal-permeability values for the steady-state 1-D flow tests



a) Comparison of various K_1 values



b) Comparison of various K_2 values

Fig. 11: Comparison of the principal-permeability values from the transient radial-flow tests and the CFD simulation.

standard-deviation values indicate that results from the experimental trials were quite close.

Results from individual radial steady-state experiments are shown in Fig. 12a and 12b. Again, limited number of trials were performed, though the results are still presented as a possible indication of the outcome of further testing. Though more data points are necessary to make these results more acceptable statistically, observations from these results will be made for what they are. If one strictly considered the results for K_2 , there seems to be some agreement between the experimental and simulated results: the average experimental value is in some agreement with the simulated value. However, the K_1 values from both trials are significantly higher than the value obtained through simulation. Because calculations for principle permeabilities are not independent, the discrepancy observed in K_1 values perhaps devalues the agreement observed for K_2 values.

Though these results are not consistent with the simulation results, the cause for the discrepancies

may be the same that caused the scatter in values obtained at low flow rates for the one-dimensional steady-state experiments. Pressures measured at the radial pressure-transducers were similar to those recorded at the low-flow rates during the one-dimensional steady-state tests. As mentioned before, the pressure transducers used lose sensitivity at low pressures. Inaccurate pressure readings at such low pressures could explain the discrepancies in measured and numerically-obtained permeability values for the steady-state radial-flow tests. The pressure transducer at the center of the radial flow mold read pressures closer to those of the higher flow-rates in the one-dimensional flow tests and was, therefore, not as affected by this effect. Furthermore, because the transient radial-flow calculations depend only on the pressure transducer at the inlet, these tests would not be affected. Indeed, the values from the transient radial-flow tests showed agreement with the values obtained through simulations.

Validity of these experimental results is based on the assumption that permeability values of the reference material obtained from CFD simulations are correct. This in mind, it is worth making an overall comparison of all the experimental results with the simulation results.

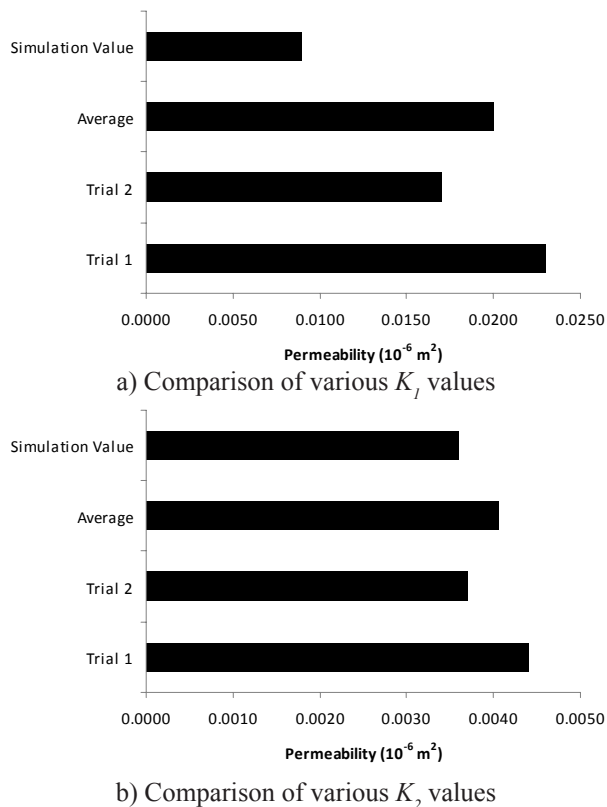


Fig. 12: Comparison of the principal-permeability values from the steady-state radial-flow tests and the CFD simulation.

Although there were limited number of trials for all but the one-dimensional steady-state tests, results for each trial for the other three tests were consistent (i.e., the calculated permeability values were consistently higher than the simulation values through all trials of a particular test). Considering the results for the transient 1-D flow evaluation of K_1 and the steady-state radial-flow evaluation of K_1 , both estimate a value of K_1 higher than that obtained through simulation. However, before concluding that K_1 is actually higher than estimated by simulation results, one should also note that for these two tests, one showed a value of K_2 higher than the value from simulation, while the other showed agreement with the simulation value. Discrepancy of the results of these two tests with each other and with the values from simulation weakens the validity of these results. However, if one considers the results of the 1-D flow tests and the transient radial-flow tests,

all show good agreement with the values obtained through simulation. Even though there were not many trials of the transient radial-flow test, there were several trials of the 1-D flow tests which displayed consistent results. So based on these overall results, we conclude that both the transient and steady-state versions of the 1-D and radial flow experiments were able to estimate values of K_1 and K_2 that were quite close to the 'exact' simulation values—the only outlier was the K_1 estimation by the steady-state radial-flow test. This implies that the exact permeability of the calibration tool can be considered known, and hence such a tool can be confidently used for future calibrations.

An important question in this work is the effect of the boundary between the rectangular part and the circular adapter during the radial-flow tests. There are two signs that the boundary had minimal influence on the results. First, visual observation during the experiment indicates that there is no interruption in the elliptically-shaped flow-front when it reaches this boundary; the flow front continues as if no boundary existed. Secondly, the results of the transient radial-flow tests closely match those from the 1-D flow tests and those from the CFD simulations. Measurements taken during the transient experiment included times both before and after the flow front passed through the boundary and, therefore, would be affected by the boundary if the boundary influenced the flow front at all. These observations serve as evidence that the method of using a circular adapter with the calibration tool from a one-dimensional experiment in order to save cost and time is valid.

Another consideration for this work is the effect of the non-circular outer-boundary of the reference medium for the radial-flow tests. As mentioned before, the entire structure was composed of full unit-cells. Therefore, a circular border was approximated with the patterning of the unit cells, but, again, it was not perfectly circular. Unfortunately this work could not provide evidence whether this affected the outcomes or not. Some results from the steady-state radial experiments did not show agreement with the simulation results, possibly a result of the effect of

this stepped border.

As was mentioned in the introduction, Roy *et al.* [7] and Hua *et al.* [8] noted a deterioration in the accuracy of their calibration devices at higher flow-rates due to an increase in mold deflections due to higher inlet-pressures. However, as seen from the results of Fig. 10, such an effect was not evident for the present reference medium—the permeability values K_1 and K_2 remained virtually constant as the liquid injection-rate was raised to four-times the starting value. Hence we can conclude that the accuracy of the reference medium remains unaffected by the magnitude of injection flow-rates. An explanation for this insensitivity can be offered. The use of rubber gaskets on top and bottom of the calibration tool provides a certain compressibility to the composite medium created for calibration. Presence of pre-stress in such a medium can absorb minute deviations inevitable at higher injection-rates and prevents springing of leaks from the sides of the reference medium. (Such leaks were observed by both Roy *et al.* [7] and Hua *et al.* [8] for their hard reference-media and could be reduced, if not eliminated, only through an extensive use of caulks and C-clamps.)

7. CONCLUSIONS

Based on discussions in the last section, the following are the valuable outcomes of this work. First, for the first time a cost-effective and accessible calibration tool has been introduced for use in both one-dimensional and radial flow permeability evaluation test apparatus. Close agreement between the permeability values obtained from CFD simulations and three of the four evaluation methods used here indicate this to be a valuable tool in assessing the accuracy of a permeability measuring device and method. Furthermore, results from tests indicate that the boundary created by pairing a rectangular part with a circular adapter does not affect the test results.

Additionally, and what is most valuable, this paper has demonstrated how the usage of this calibration tool can lead to not only an understanding of the strengths of an experimental set-up but also to

possible reasons for inaccuracies during its setup. From the previous discussions, a plausible explanation for the scatter in data at low flow-rates for the 1-D steady-state tests and inaccuracy of the radial steady-state tests is developed. This may be further tested by performing the radial steady-state experiments at higher flow-rates and, consequently, higher pressures.

Similarly the general insensitivity of the tool accuracy to an increase in flow rates was noted. Hence, testing of this reference medium under different conditions can be very enlightening and useful to experimenters using the 1-D and radial flow devices.

In the future, these conclusions can be strengthened not only by further testing using the same equipment that was used for these experiments, but also by testing by others using different experimental set-ups. This calibration tool is very accessible and customizable, making it an attractive option for creating a standard reference medium with which to analyze and compare experimental set-ups for their permeability estimation capabilities.

ACKNOWLEDGEMENTS

We would like to thank the College of Engineering and Applied Science at the University of Wisconsin–Milwaukee and the National Science Foundation (U.S.A.) for providing funding through their undergraduate research award and through grant # 0348097, respectively, to support this research. We would like to thank Mr. Morren and Professor Lomov for being so helpful in providing details of their reference media as well as their work with it. We would also like to thank Mr. Hua Tan for his input throughout this project.

Nomenclature

English letters

A	Flow front Cross-sectional area [m ²]
d	Characteristic width of porous media [m ²]
f	A parameter {Eqns. (6) and (7)}
h	Thickness of the preform [m]
K	Permeability tensor [m ²]
K	Permeability [m ²]
L	Length of the material [m]
P	Pressure

P_o, P_1, P_2	Pressures measured by the central, first and second pressure transducers {Eqns. (12) and (13)}
q	Darcy velocity {Eq (1)}
Q	Flow rate [m ³ /s]
r	Radius [m]
r_o	Radius of the inlet hole
Re	Reynolds number
t	Time [s]
V	Velocity [m/s]
x_1	x-location of the first pressure transducer {Eq (12)}
y_2	y-location of the second pressure transducer {Eq (13)}

Greek Letters

μ	Dynamic viscosity of the liquid [kg/m.s]
ε	Porosity
ρ	Fluid density [kg/m ³]
α	A parameter {Eqns. (7) and (8)}
	Gradient operator

Subscripts

0	Initial value
1	Corresponding to the first principle direction of K tensor {Eqs (6)-(8)}
2	Corresponding to the second principle direction of K tensor {Eqs (6)-(8)}
eff	Effective
$front$	liquid front
$inlet$	Inlet
$outlet$	Outlet
ss	Steady state
tr	Transient
xx	xx component of a second order tensor {Eq (2)}
xy	xy component of a second order tensor {Eq (2)}
yx	yx component of a second order tensor {Eq (2)}
yy	yy component of a second order tensor {Eq (2)}

References:

1. Baichen, L., Bickerton, S., and Advani, S.G., "Modeling and Simulation of Resin Transfer Moulding (RTM) – Gate Control, Venting and Dry Spot Prediction", *Composites: Part A*, **27A** (1996), 135-141.

2. **Gauvin, R., Trochu, F., Lemenn, Y., and Diallo, L.,** "Permeability Measurement and Flow Simulation Through Fiber Reinforcement", *Polymer Composites*, **17/1** (1996), 34-42.
3. **Hoes, K., Dinescu, D., Sol, H., Parnas, R.S., Lomov, S.,** "Study of Nesting Induced Scatter of Permeability Values in Layered Reinforcement Fabrics", *Composites: Part A*, **35** (2004), 1407-1418.
4. **Parnas, R.P., Howard, J.G., Luce, T.L., and Advani, S.G.,** "Permeability Characterization. Part 1: A Proposed Standard Reference Fabric for Permeability", *Polymer Composites*, **16/6** (1995), 429-445.
5. **Parnas, R.S., Flynn, K.M., and Dal-Favero, M.E.,** "Permeability Database for Composites Manufacturing", *Polymer Composites*, **18/5** (1997), 623-633.
6. **Lundstrom, T.S., Gebart, B.R., and Sandlund, E.,** "In-Plane Permeability Measurements on Fiber Reinforcements by the Multi-Cavity Parallel Flow Technique", *Polymer Composites*, **20/1** (1999), 146-154.
7. **Roy, T., Tan H., and Pillai, K.M.,** "A Method To Estimate The Accuracy Of 1-D Flow Based Permeability Measuring Devices", *Journal of Composite Materials*, **41/17** (2007), 2037-2055.
8. **Tan H., and Pillai, K.M.,** "A method to estimate the accuracy of radial flow based permeability measuring devices", *Journal of Composite Materials*, **43/21** (2009), 2307-2332.
9. **Morren, G., Gu, J., Sol, H., Verleye, B., and Lomov, S.,** "Stereolithography Specimen To Calibrate Permeability Measurements For RTM Flow Simulations", *Advanced Composites Letters*, **15/4** (2006), 119-125.
10. **Verleye, B.,** "Computation Of The Permeability Of Multi-Scale Porous Media With Application To Technical Textiles", Thesis, Departement Computerwetenschappen Celestinjenlaan, Katholieke Universiteit Leuven, March 2008.
11. **Chan, A.W., Larive, D.E., and Morgan, R.J.,** "Anisotropic Permeability of Fiber Preforms: Constant Flow Rate Measurement", *Journal of Composite Materials*, **27/10** (1993), 996-1008.
12. **Wang, T.J., Wu, C.H., and Lee, L.J.,** "In-Plane Permeability Measurement and Analysis in Liquid Composite Molding", *Polymer Composites*, **15/4** (1994) 278-288.
13. **Gebart, B.R. and Lidstrom, P.,** "Measurement of in-Plane Permeability of Anisotropic Fiber Reinforcements", *Polymer Composites*, **17/1** (1996), 43-51.
14. **Han, K.K., Lee, C.W., Rice, B.P.,** "Measurements Of The Permeability Of Fiber Preforms And Applications", *Composites Science and Technology*, **60** (2000), 2435-2441.
15. "FineLine Prototyping", <http://www.finelineprototyping.com/>.
16. National Instruments Inc., <http://www.ni.com/data-acquisition/>.
17. **Wheeler, A.J. and Ganji, A.R.,** *Introduction to Engineering Experimentation*, Second Edition, Pearson Prentice Hall.